

Article

Tuning the Wettability of a Commercial Silane Product to Induce Superamphiphobicity for Stone Protection

Panagiotis N. Manoudis ¹, Zebunnisa Chughtai ¹, Vasilios Tsiridis ², Sotiris P. Evgenidis ¹,
Panagiotis K. Spathis ¹, Thodoris D. Karapantsios ¹ and Ioannis Karapanagiotis ^{1,*}

¹ Department of Chemistry, Aristotle University of Thessaloniki, GR-54124 Thessaloniki, Greece

² Department of Civil Engineering, Aristotle University of Thessaloniki, GR-54124 Thessaloniki, Greece

* Correspondence: karapana@chem.auth.gr

Abstract: Silane-based materials are used for the protection of heritage and modern buildings. A versatile method is developed to tune the wetting properties of a typical silane-based material from hydrophobicity to superamphiphobicity, thus enhancing the protective efficacy against rainwater and organic pollutants. A commercially available silane product is blended with a fluoropolymer to lower the surface energy and silica (SiO₂) nanoparticles to affect the surface morphologies of the produced coatings on marble. Contact angles of water and oil drops are measured on the coating surfaces which were prepared using 16 different combinations of fluoropolymer and nanoparticle concentrations. It is shown that the synergistic effect of surface structure and chemistry can lead to the production of coatings that possess superamphiphobic properties. The wetting properties of a selected non-wettable coating are further characterised using a custom-made, fully-automated device (*Kerberos*) which monitors simultaneously the deformation of the liquid interface, spreading and sliding of the drop along the sample surface during tilting. Several tests are carried out to evaluate the durability of the selected superamphiphobic coating, offering overall promising results. The versatile method can be used to impart superamphiphobicity to the surfaces of various materials. The method developed herein can be adopted to tune the wetting properties of other silane-based commercial products which are used for the protection of buildings.

Keywords: superhydrophobic; superoleophobic; superamphiphobic; stone; heritage



Citation: Manoudis, P.N.; Chughtai, Z.; Tsiridis, V.; Evgenidis, S.P.; Spathis, P.K.; Karapantsios, T.D.; Karapanagiotis, I. Tuning the Wettability of a Commercial Silane Product to Induce Superamphiphobicity for Stone Protection. *Coatings* **2023**, *13*, 700. <https://doi.org/10.3390/coatings13040700>

Academic Editor: Enrico Quagliarini

Received: 25 February 2023

Revised: 18 March 2023

Accepted: 27 March 2023

Published: 30 March 2023



Copyright: © 2023 by the authors. Licensee MDPI, Basel, Switzerland. This article is an open access article distributed under the terms and conditions of the Creative Commons Attribution (CC BY) license (<https://creativecommons.org/licenses/by/4.0/>).

1. Introduction

Silane/siloxane-based products are commonly used for the conservation of natural stone and stone-built cultural heritage, because they possess three important properties: high depth of penetration, stability, and hydrophobicity [1,2]. Polysiloxane networks originate from small precursor molecules of silanes and siloxanes which can penetrate deep into the stone network before they become highly viscous gels (i.e., polysiloxanes) through the sol-gel process [3]. Consequently, higher depths of penetrations are achieved by the silane-based consolidants, compared with the high molecular weight organic polymers which correspond to high viscosity and were used in the past for stone consolidation [4–7]. Polysiloxane materials are often considered as hybrid materials because their backbone chains are formed by the siloxane (Si-O) bond which is of “inorganic” nature, while the substituents attached to the Si atom are generally “organic” radicals [8]. Due to their dual nature, polysiloxane compounds possess stability and hydrophobicity. Stability originates from the high strength of the Si-O bond compared with the C-C bond which forms the backbones of organic polymers. In particular, the strengths of the Si-O and C-C bonds correspond to 108 and 83 kcal/mol, respectively [1]. High Si-O bond strength offers siloxane-based materials with considerable thermal stability as well as good corrosion and UV resistance [1,9,10].

Hydrophobization of natural stone surfaces is a practical method to impede water-induced degradation of buildings of cultural heritage. Typical organic polymers used in

the past [11–13] possess hydrophobicity but they fall short either on stability or the desired depth of penetration. The inherent hydrophobic character of the siloxane-based materials originates from the organic groups which are attached to the Si atoms of the backbone chain. The contact angle of a water drop (WCA) on a very smooth polysiloxane surface, produced for instance by spin coating on a smooth glass substrate, is typically on the order of 100° . This value, however, can be highly increased if the polysiloxane coating is produced and deposited on the surface of a rough stone substrate. Because the surface of the underlying stone substrate is rough, the surface of the deposited polysiloxane coating becomes also rough. [14]. As the surface roughness of an inherently hydrophobic material increases, so does the WCA according to the Wenzel [15] and Cassie-Baxter [16] models. Hence, poly(alkyl siloxane) coatings which were produced using Rhodorsil 224 and were deposited on smooth glass, slightly rougher marble, and very rough sandstone, gave WCAs of 103° , 108° , and 141° , respectively [14,17].

Roughness induced by the substrate morphology to the surface of a typical polysiloxane is not capable to achieve the extreme threshold of superhydrophobicity (WCA $> 150^\circ$). Carefully designed synthetic routes should be implemented to produce a highly rough topography on the coating surface. For example, a superhydrophobic coating was produced on marble, sandstone, granite, and travertine using a sol of methyltrimethoxysilane and appropriate reagent concentrations to control the sol-gel process which led to the formation of a micro/nano-structured coating surface [18]. Following the example of the famous lotus leaf [19], the synergistic effect of high roughness and low surface energy agent (e.g., a fluoropolymer) can be effective to achieve non-wetting properties on the surfaces of treated stones. Aslanidou et al. produced a coating using an emulsion of alkoxy silanes and organic fluoropolymer (Silres BS29A) [20]. The coating possessed superhydrophobic properties when it was deposited on rough sandstone but not on smooth marble [20]. Adamopoulos et al. [21] deposited a sol of co-hydrolysed TEOS and a fluorinated agent on marble and other materials which obtained superhydrophobicity.

In another, more flexible method which was devised to produce superhydrophobic coatings on natural stone, engineering nanoparticles (NPs) are added to the silane/siloxane sol [22]. The composite (polysiloxane + NPs) coating which is produced on the stone surface after sol deposition is very rough because the presence of the NPs leads to the formation of surface protrusions [22]. As the effect of the high surface roughness on the wetting properties is dominant, the use of a low surface energy agent is not necessary to achieve superhydrophobicity. Following this method, the wetting properties of several commercially available silane/siloxane conservation products such as Porosil VV Plus [14], Rhodorsil 224 [14,17,23,24], Silres BS 4004 [25], TES 40 WN [26,27], Silres BS29A [20,28], Dynasytan F8815 [29], ESTEL1100 [30], Alpha[®]SI30 [31], Dynasytan 40 [32] and Silres BS38 [33] were tuned to enhance their hydrophobic character, achieving in most cases superhydrophobicity [14,17,23–25,27–31].

The combined oleophobicization and hydrophobization of natural stone surfaces are highly desirable to protect buildings of cultural heritage that are threatened by oil-based pollutants, particularly in urban areas. This combination is realized on superamphiphobic surfaces which have the ability to repel both water and oil i.e., both water (WCA) and oil (OCA) contact angles are $>150^\circ$. Producing a superamphiphobic silane-based coating is a challenging task. Typically, silane-based materials can lead to superhydrophobicity when they are mixed with NPs, as described above, but they cannot resist the wetting of organic liquids. Hence, the production of superamphiphobic coatings on natural stone was achieved in very few studies. In particular, Silres BS29A + NPs [20,28] and 3-perfluoroetheramidopropylsilane [34] exhibited superamphiphobicity when they were deposited on natural stone.

A method that can be used to tune the wetting properties of a typical silane-based material from hydrophobic to superamphiphobic is presented herein. The polysiloxane network originates from a commercially available aqueous silane solution (Protectosil SC Concentrate). The silane product is blended with a fluoropolymer to lower the surface

energy and silica (SiO₂) nanoparticles (NPs) to induce surface roughness. Composite coatings are deposited on marble specimens. The latter was selected as substrates because the marble surface is relatively smooth (compared with other natural stones) and therefore its effect on the morphology of the coating surface is negligible. It is shown that careful selection of the appropriate fluoropolymer and NP concentration leads to surfaces of extreme wetting properties with both WCA and OCA being >150°. A superamphiphobic surface is selected and studied further using a custom-made, fully-automated device that monitors simultaneously the deformation of the liquid interface, the spreading and sliding of the drop along the sample surface during tilting. A number of different tests are carried out to evaluate the durability of the selected superamphiphobic surface. The developed method can be used as a roadmap to improve the wetting properties of other silane-based materials which are provided for the protection of building materials. These commercial silane-based products exhibit typically hydrophobic properties. We show that when such a product is blended with a low surface energy agent (fluoropolymer) to affect surface chemistry and NPs to affect surface morphology, the resulting coating obtains superamphiphobic properties, thus offering superior protection compared with the typical hydrophobic materials.

2. Materials and Methods

According to the manufacturer (Evonik, Essen, Germany), Protectosil SC Concentrate (P) is an aqueous solution based on silane chemistry that is recommended for the treatment of mineral substrates, including marble. The product was diluted in demineralized water to prepare two solutions with concentrations 6% *w/w* (6P) and 1% *w/w* (1P). A water-based fluoropolymer (Ruco-Guard Air 6, Rudolf, Germany, C6 fluorocarbon polymer, cationic) emulsion (F) was provided by Lysis Consulting (Pylaia, Greece) and was added to the 6P and 1P solutions. Three sols were produced using different concentrations of the two, P and F, products as described in Table 1. The 6P solution was included in the study (Table 1).

Table 1. Aqueous sols which were prepared and used in the study to treat marble.

Abbreviation	Sols & Concentrations
6P	6% <i>w/w</i> Protectosil
6P/1F	6% <i>w/w</i> Protectosil & 1% <i>w/w</i> Fluoropolymer
6P/6F	6% <i>w/w</i> Protectosil & 6% <i>w/w</i> Fluoropolymer
1P/6F	1% <i>w/w</i> Protectosil & 6% <i>w/w</i> Fluoropolymer

Fumed silica (SiO₂) nanoparticles (Aldrich) with a 7 nm mean diameter were dispersed in the four sols of Table 1, at three different concentrations: 1, 2, and 3% *w/w*. Therefore, twelve dispersions were produced in total using different relative concentrations of P, F, and SiO₂. Dispersions are named using the abbreviations of the sols followed by the % *w/w* concentration of the SiO₂ NPs which are designated by “Si”. For example, the 6P/1F/2Si dispersion was prepared using 6% *w/w* P, 1% *w/w* F and 2% *w/w* SiO₂ NPs. The abbreviations of the twelve dispersions are described in detail in Table S1 of the Supplementary Materials. In sum, sixteen coatings were produced in total on marble, by varying the relative concentrations of SiO₂ NPs which were added to the sols of Table 1.

The deposition of the dispersions onto smooth marble surfaces was carried out using an airbrush system (Paasche Airbrush) with a nozzle diameter of 733 µm, which was held at a distance of 20 cm from the marble surface. Immediately after preparation, the dispersions were stirred vigorously for 30 min and were then sprayed for 2 s onto the marble specimens. Samples were left to cure and dry at 70–80 °C for 1 h and then at room temperature for 24 h. The sample preparation process is shown in Figure 1.

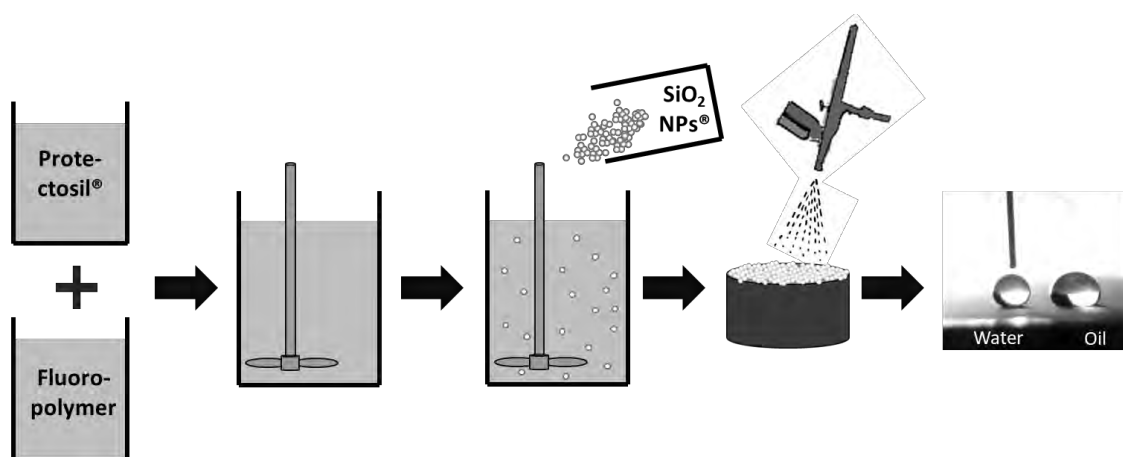


Figure 1. Schematic presentation of the method which was applied to produce superamphiphobic coatings on marble.

Drops (8 μL) of distilled water and olive oil (purchased from the local market) were placed onto coated marble samples and contact angles were measured using the ImageJ software. The reported static contact angles of water (WCA) and oil (OCA) drops as well as the reported contact angle hysteresis are averages of five measurements. Scanning electron microscopy (SEM; TM3000, HITACHI; Tokyo, Japan) was employed to study the surface structures of the treated marble samples at the micrometer scale. SEM (Jeol JSM-IT500; Tokyo, Japan) was used to collect high magnification SEM images and to characterise the two additives which were used to affect the wetting properties of the silane product (P), which are the fluoropolymer (F) and the SiO_2 NPs. Characterisation was completed using an energy-dispersive X-ray (EDS) microanalytical system and the results are shown in Figures S1 and S2 of the Supplementary Materials.

The dynamic behaviour of water drops on 6P/1F and 6P/1F/2Si during titling, has been recorded using a custom-made, fully-automated device, called *Kerberos*. The instrument uses synchronized Wi-Fi cameras to monitor the deformation of the liquid interface, the spreading and sliding of the drop along the sample surface during tilting. Obtained videos were post-processed by means of a custom image processing software to extract a number of 2-dimensional drop geometrical features (i.e., contact angles, drop length, height, width, etc.), as well as the 3-dimensional reconstruction of the drop shape. More information on the *Kerberos* device can be found in previous studies that presented in detail the working principles and the technical specifications of both hardware and software, along with results obtained using reference solid surfaces such as glass and PTFE [35–37]. In the present study, experiments were conducted for sample tilting from 0° to 50° with a constantly increasing rate of $0.25^\circ/\text{s}$, at a temperature of $25 \pm 2^\circ\text{C}$ and relative humidity of $50 \pm 5\%$.

The 6P/1F and 6P/1F/2Si surfaces were subjected to several tests to evaluate their stability on a comparative basis. In particular, drops of solutions, which were prepared using hydrochloric acid (HCl, ChemLab) and sodium hydroxide (NaOH, ChemLab) and corresponded to a pH range from 0 to 14, were placed on the surfaces and contact angles were measured. For the artificial ageing under UV radiation, samples were placed inside a chamber, equipped with UV source (Osram Dulux S Blue, 9W/78V, UVA 300–400 nm). The temperature in the chamber was kept at 27.7°C , the radiation intensity was 1.064 W/m^2 and the distance between the sample surface and the UV lamp was 32 cm. Contact angles were measured periodically during the 18-week period of treatment. For the rain simulation test, samples were placed under a container filled with distilled water. The container had four small holes at the bottom, allowing small drops to fall and hit the sample surface. The distance between the bottom of the container and the sample surface was 50 cm, while a total amount of 2 L of water dropped on the sample surface at a rate of 1 L/h.

Samples were then dried at 60 °C in an oven for 2 h and contact angles were measured. The same test protocol was followed to simulate acid rain which was realized using a water solution with a pH of 4.3. For the freeze-thaw test, coated marbles were subjected to a freezing temperature of −22 °C for 15 min and then thawed inside a silica desiccator to room temperature [38]. The procedure was repeated 15 times (cycles). Finally, the tape peeling test was carried out using a Scotch Tape 600 (3M) according to the ASTM D3359 97 standard test (method A). Thirty (30) cycles were applied in total. The aforementioned measurements were carried out in triplicate in three different areas of sample surfaces.

3. Results

3.1. Discrete Effects of Surface Structure and Surface Chemistry on Wettability

The WCAs and OCAs, measured on the surfaces of the coatings which were prepared using the silane product (P), enriched only with NPs are shown in Figure 2a. Fluoropolymer (F) was not included in the surfaces of Figure 2a. The WCAs and OCAs, measured on the surfaces of the coatings which were prepared using P enriched only with F, are shown in Figure 2b. NPs were not included in the surfaces of Figure 2b. In the following, attention focuses first on Figure 2a whereas the results of Figure 2b are discussed later.

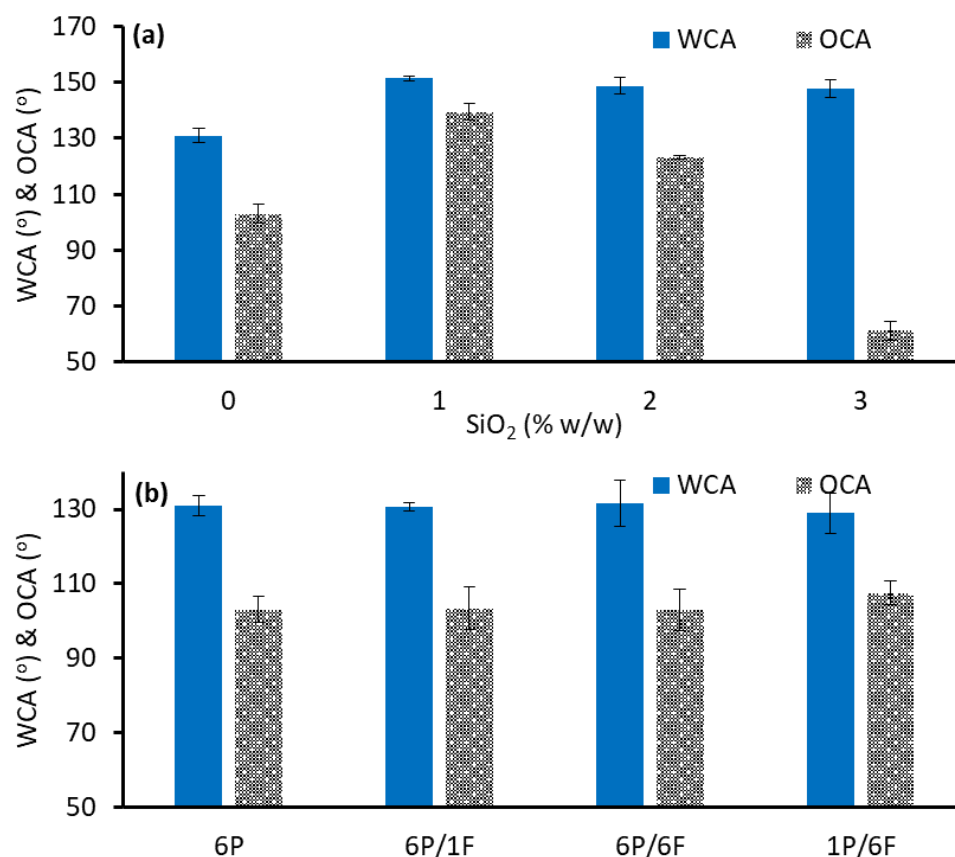


Figure 2. (a) WCA and OCA vs. SiO₂ NP concentration for the 6P-based coatings (F was not used). (b) WCA and OCA on surfaces of which were prepared by blending P and F in different ratios (NPs were not used).

The 6P coating which was produced using only the silane product showed an enhanced hydrophobicity (WCA = 131.0°) and weak oleophobicity (OCA = 103.0°). According to the results of Figure 2a, the hydrophobic character of the coating was promoted with the addition of the NPs, reaching barely the threshold of superhydrophobicity. Considering the variations reported in Figure 2a, the WCAs on the 6P/1Si, 6P/2Si, and 6P/3Si surfaces were roughly the same and on the order of ~150°. The corresponding variation of OCA is more complicated. Initially, OCA increased from 103.0° (on 6P surface) to 139.5° (on 6P/1Si

surface). Further increase in the NP concentration leads to a rapid decrease in OCA to 123.2° (on 6P/2Si surface) and 61.2° (on 6P/3Si surface). Interestingly, the same variations of WCA and OCA with NP concentration were observed by Aslanidou et al. [20] who produced composite coatings using Silres BS29A and SiO_2 NPs [20]. These variations are discussed next in light of the SEM images of Figure 3 which reveal the effect of the NPs on the surface structures of the produced coatings.

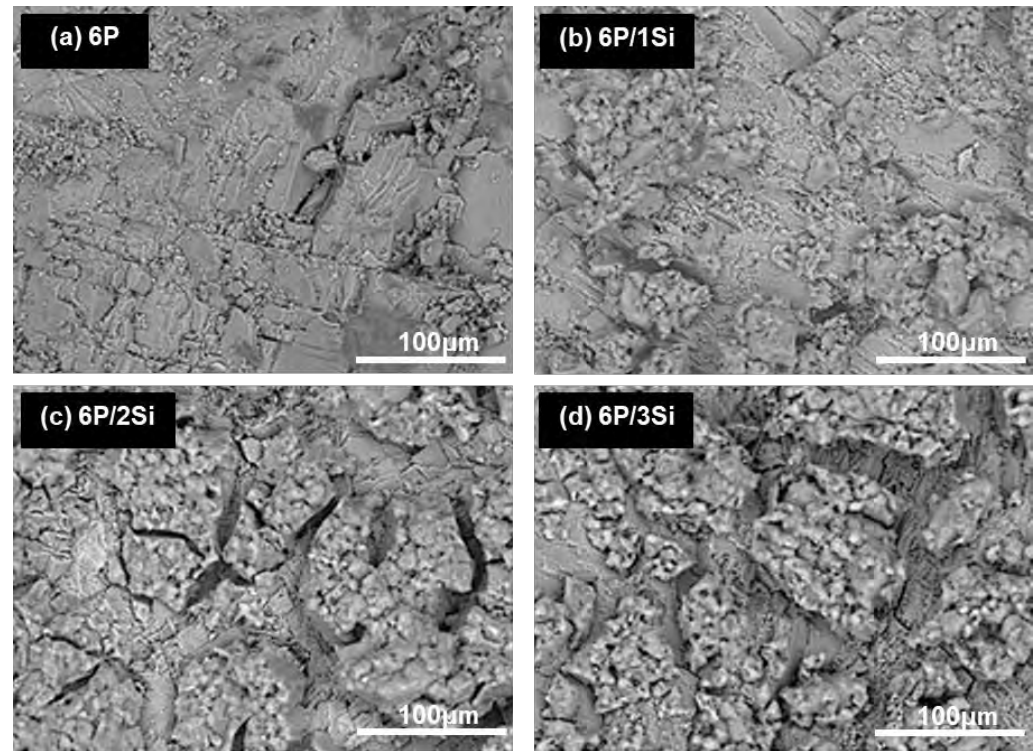


Figure 3. Surface structures of the 6P-based coatings, which were prepared using (a) no NPs (b) 1, (c) 2 and (d) 3% *w/w* NP concentration. Fluoropolymer F was not included.

The 6P surface, which was produced without using NPs, was relatively smooth with some features originating from the substrate roughness (Figure 3a). A small number of NPs (1% *w/w*) resulted in the formation of a rough surface 6P/1Si (Figure 3b) which gave rise to both WCA and OCA (Figure 2a). This increase in contact angles with surface roughness is supported by the Cassie-Baxter model [16]:

$$\cos CA = -1 + f_S(\cos CA_S + 1) \quad (1)$$

where CA_S is defined for an atomically smooth surface, CA is the contact angle on the rough surface and f_S is the solid fraction contacted by the liquid. As roughness increases, the f_S factor decreases, giving rise to the apparent CA . According to the SEM image of Figure 3c, a network of large protrusions separated by grooves was formed in the composite coating when the NP concentration became 2% *w/w* (6P/2Si surface) followed by a reduced OCA (Figure 2a). Combining the data of OCAs (Figure 2a) and surface structures (Figure 3b,c) it is suggested that the oil drops sank into the grooves which were formed on the 6P/2Si surface, resulting in a decreased OCA. Further increase in the NP concentration (6P/3Si surface) resulted in larger grooves (Figure 3d), thus making the oil drop collapse more dramatic which led to a further decrease in OCA (Figure 2a). Water has a much higher surface tension ($=72 \text{ mN/m}$) than oil ($=32 \text{ mN/m}$). Consequently, the drops of water did not collapse because of the elevated Laplace pressure. Water drops could stay suspended on the protrusions and therefore the effect of the grooves on WCA was practically negligible

(Figure 2a) although a very slight reduction of the reported WCAs can be noticed as the NP concentration increases from 1 to 3% w/w .

According to the results reported in Figure 2b, F had practically no effect on the WCA of the P-based coatings. In particular, the WCAs on the 6P, 6P/1F, 6P/6F, and 1P/6F surfaces were comparable and varied slightly around the value of $\sim 130^\circ$. In sum, the WCAs on 6P and 6F surfaces were not significantly different and therefore the coatings which were prepared using different mass ratios of P and F showed similar WCAs. F had a slight but statistically noticeable effect on the OCA of the P-based coatings. As shown in Figure 2b, OCA increased with the amount of F, which was added to the coatings, from 103.0° (6P surface with no F) to 107.5° (1P/6F surface which corresponds to the maximum amount of F). While the OCA on marble specimens coated with 6P was $103.0 \pm 3.5^\circ$ (Figure 2b), the OCA on marble specimens coated with 6F was $109.8 \pm 3.7^\circ$ (not included in Figure 2b). Consequently, the oleophobic characters of the P and F materials are not very much different, but according to the results of Figure 2b, this led to a slight but noticeable effect on the reported values of OCA.

Summarising the aforementioned discussion and results, it is reported that roughening the surface of the silane product using NPs led to (i) weak and delicate superhydrophobicity which can be easily lost if the NP concentration is not selected carefully and (ii) enhanced oleophobicity without, however, reaching the demanding threshold for superoleophobicity ($OCA > 150^\circ$). On the other hand, lowering the surface energy of the produced coating by adding a fluoropolymer into the silane product (i) had practically no effect on WCA which, however, was kept at the elevated value of around 130° and (ii) led to a very slight, but noticeable, increase in OCA. It is stressed that these results are reported for the relative concentrations of the P and F products (Table 1) which were investigated in this study. In the following, it is shown that the synergistic effect of surface structure and surface chemistry can lead to the production of coatings that possess superamphiphobic properties.

3.2. Synergistic Effect of Surface Structure and Surface Chemistry on Wettability

The synergistic effect of surface topography and chemistry is necessary to achieve superamphiphobicity, as discussed in a recently published review [39]. The cross-influence effects of surface chemistry and morphology on WCA and OCA are revealed in Figure 4a,b, respectively. In Figure 4 only the mean values of WCA and OCA are shown whereas the corresponding variations are included in Tables S2 and S3 of the Supplementary Materials. Furthermore, the results reported in Figure 2 are reproduced in Figure 4. The latter shows that the addition of a small amount (1% w/w) of SiO_2 NPs to any of the four sols of Table 1 leads to an increase in WCA, compared with the results reported for the corresponding surfaces which were prepared without using SiO_2 NPs. The WCA on the four coatings which were enriched with 1% w/w NPs ranged between 151.0 – 153.8° , thus suggesting that superhydrophobicity was achieved. For the same four coatings (with 1% w/w NPs), OCA corresponded to elevated values, ranging from 139.5° (6P/1Si surface) to 145.6° (either 6P/6F/1Si or 1P/6F/1Si surfaces). Moreover, the results of Figure 4 show that the elevation of the NP concentration to 2% w/w , increased both WCA and OCA ($>150^\circ$) on the surfaces which contained the low surface energy agent, F. Therefore, superamphiphobicity was achieved on the 6P/1F/2Si, 6P/6F/2Si and 1P/6F/2Si surfaces. However, as described in the previous chapter, the 2% w/w concentration of NPs did not promote hydrophobicity and suppressed the oleophobic properties of the 6P-based coating which was produced without using F (i.e., 6P/2Si surface). In sum, superamphiphobic coatings were produced only when the effects of surface morphology, affected by the NP concentration, and surface chemistry, affected by F, were combined appropriately.

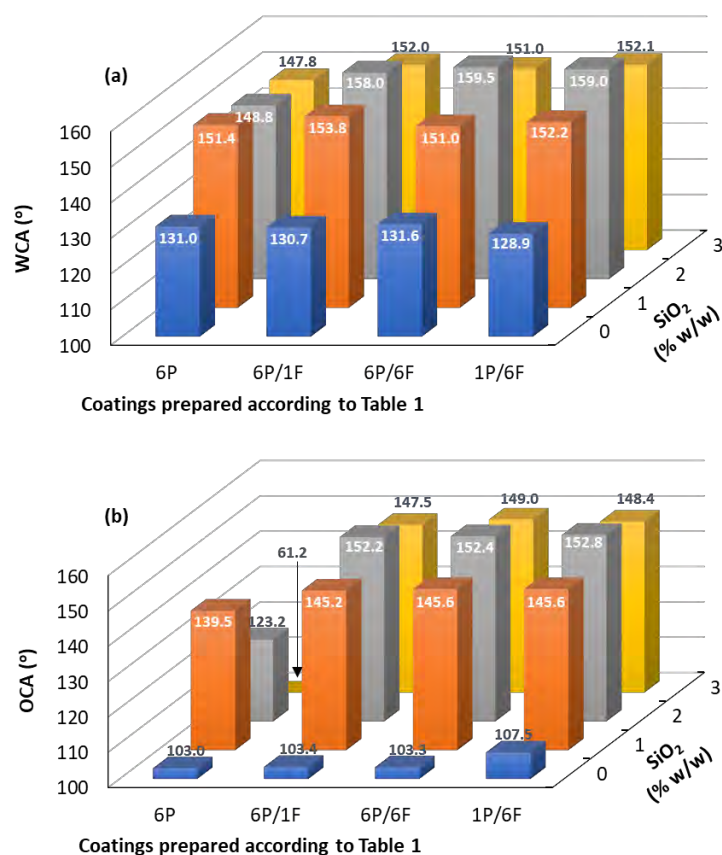


Figure 4. (a) WCA and (b) OCA on the sixteen coatings which were prepared using different P and F ratios and SiO₂ NP concentrations.

The surface structures of the 2Si-based coatings, which were prepared using 2% *w/w* SiO₂ NPs, are revealed in the SEM images of Figure 5. The morphologies of the four surfaces are similarly showing large grooves formed between large protrusions. Consequently, the increase in WCA from 148.8° (6P/2Si surface) to augmented values (158.0–159.5°) which were measured on the fluorinated surfaces (6P/1F/2Si, 6P/6F/2Si, and 1P/6F/2Si) was raised by the presence of the low surface energy agent, F (Figure 4). The effect of F on OCA was more pronounced. As described in the previous chapter, oil drops on the 6P/2Si surface sank into the large grooves, resulting in a reduced OCA (=123.2°). On the contrary elevated OCAs (>150°) were measured on the 6P/1F/2Si, 6P/6F/2Si, and 1P/6F/2Si surfaces, suggesting that oil drops could stay suspended on the protrusions of these fluorinated surfaces, water drops did on the 2Si-based surfaces, which were prepared with or without F. Consequently, lowering the surface energy of the 2Si-based coatings by adding F, made the oil drops capable to behave in the same way as the water drops did on the high surface energy 6P/2Si surface. Furthermore, the results of Figure 4 show that the relative concentrations of P and F which were used to prepare the three fluorinated 2Si-based coatings did not have any effect on their surface wettabilities. WCA and OCA on the 6P/1F/2Si, 6P/6F/2Si, and 1P/6F/2Si surfaces, varied within very short ranges from 158.0 to 159.5° and from 152.2 to 152.8°, respectively.

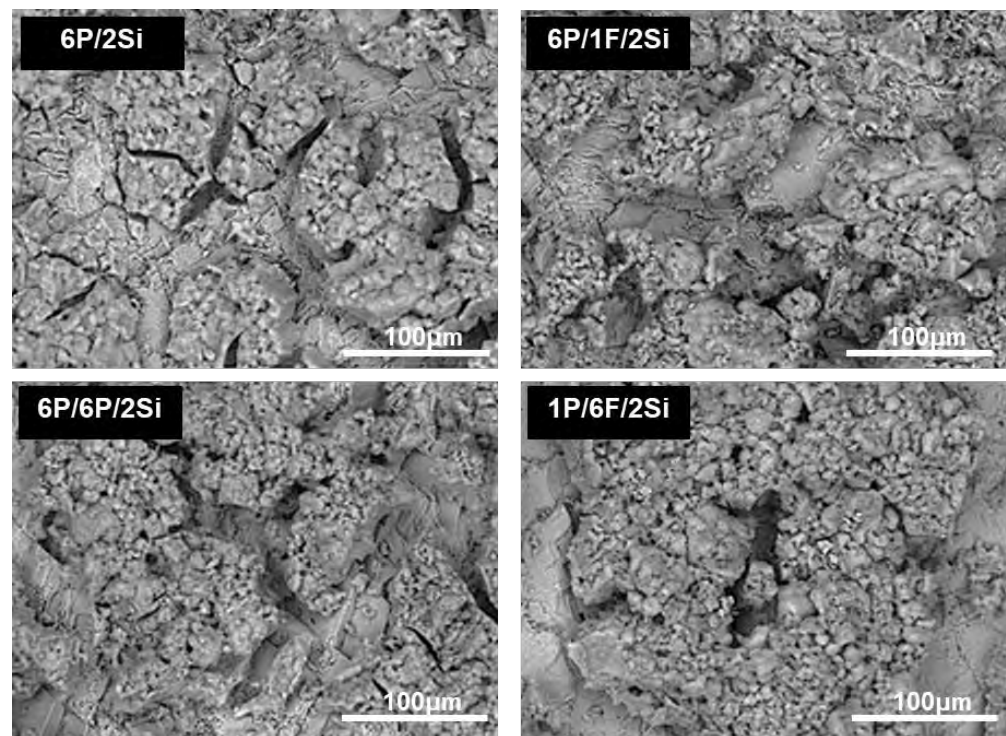


Figure 5. Surface structures of the 2Si-based coatings, which were prepared using 2% *w/w* NP concentration and different P and F ratios.

According to Figure 4, a further increase in the NP concentration to 3% *w/w* led to slight reductions of WCA and OCA on the fluorinated surfaces, compared with the results reported for the corresponding surfaces which were prepared using 2% *w/w* NPs. Superhydrophobicity was maintained on these 3Si-based fluorinated surfaces whereas superoleophobicity was almost evidenced, as OCA on the 6P/1F/3Si, 6P/6F/3Si, and 1P/6F/3Si surfaces ranged within 147.5°–149.0°. The wettability of the non-fluorinated 6P/3Si surface was discussed in the previous chapter.

Figure 6 shows high magnification SEM images of the 6P/1F/2Si surface which were taken from protruding microstructures, discussed in Figure 5. It is shown that the protrusions, which are formed at the micrometer scale, consist of nanostructures. Consequently, a two-length-scale hierarchical structure is formed on the 6P/1F/2Si surface, similar to the structure observed in the lotus leaves. Finally, a photograph showing a water and oil drop on the superamphiphobic 6P/1F/2Si surface is included in Figure 6.

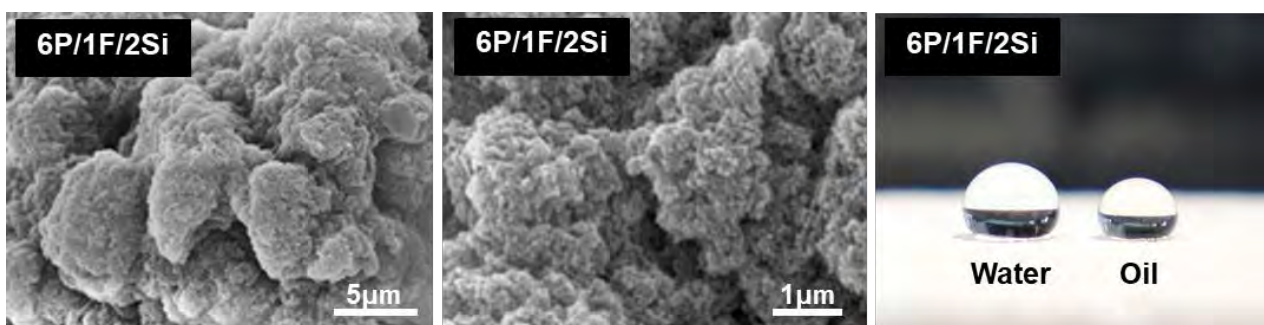


Figure 6. High magnification SEM images of the 6P/1F/2Si coating. A photograph showing a water and oil drop on the 6P/1F/2Si surface is included.

3.3. Dynamic Behaviour of Water Drops

The 6P/1F/2Si surface was selected as a typical superhydrophobic surface to study the dynamic behaviour of water drops upon titling using the custom-made Kerberos device. For comparison, the hydrophobic 6P/1F surface was included in the study. Figure 7a,b show the results for the 6P/1F surface and present the evolution of water drop contour and contact line length as a function of sample tilting. The right (rear) contact point of the drop is constantly pinned in place, as the sample inclination increases from 0 to 50°. On the contrary, the left (front) contact point moves towards the direction of the applied force leading to a clear drop-shape deformation (Figure 7a). This behaviour implies that sample tilting provokes solely spreading (and not sliding) of the drop. Moreover, the drop contact line length is almost constant up to a sample tilting of ~17° and then starts to increase progressively, indicating that drop spreading initiates around this inclination value (Figure 7b).

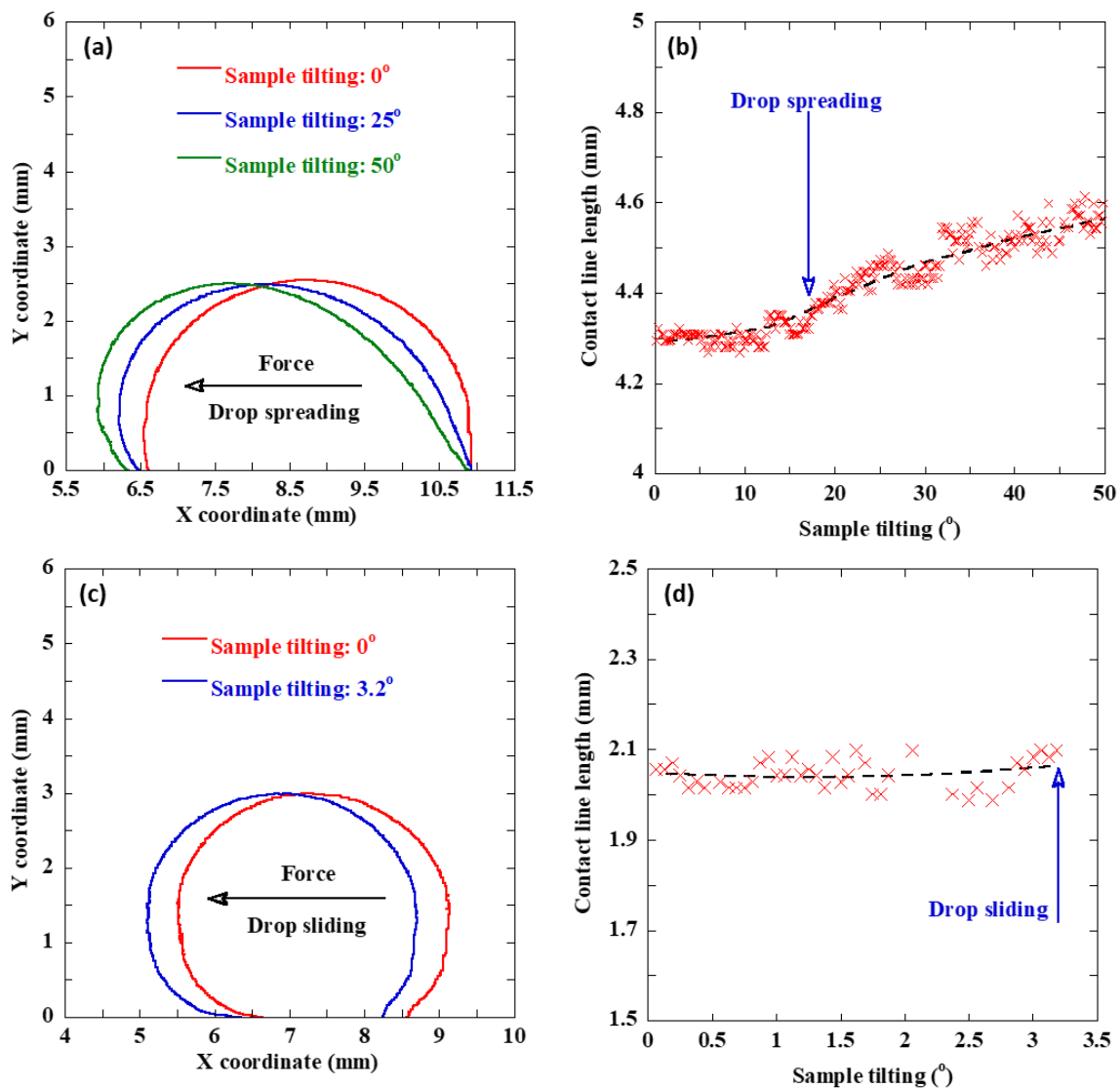


Figure 7. Evolution of water drop (a) contour and (b) contact line length as a function of tilting angle for the hydrophobic 6P/1F surface. Evolution of water drop (c) contour and (d) contact line length as a function of tilting angle for the superhydrophobic 6P/1F/2Si surface.

The results for 6P/1F/2Si surface, presented in Figure 7c,d, show the advancement of drop contour and contact line length with sample tilting increase. The addition of

SiO₂ NPs provides superhydrophobic properties to the polymeric coating and, as a result, static (sample tilting: 0°) contact angle and drop height clearly increase (Figure 7a vs. Figure 7c) and initial contact line length (sample tilting: 0°) decreases in a great extent (Figure 7b vs. Figure 7d). Figure 7c shows that even a slight sample tilting, ~3°, is enough to make drop sliding on the 6P/1F/2Si surface; both drop contact points move towards the direction of the employed force, while the drop shape does not change. In addition, the drop contact line length remains roughly constant indicating that no drop spreading takes place (Figure 7d). In sum, the results of Figure 7c,d reveal the water-repellent property of the 6P/1F/2Si surface which is evidenced in the lotus leaf-like surfaces [19]. To further demonstrate the water-repellent character of the 6P/1F/2Si surface, the self-cleaning scenario, which is typically observed in the lotus leaf-like surfaces, is shown in Figure S3 of the Supplementary Materials.

3.4. Durability Tests

The durability of the structured 6P/1F/2Si surfaces is demonstrated in Figures 8 and 9, which summarise the results of several relevant tests. The 6P/1F was included in these studies for comparison. In particular, Figure 8a shows that WCA is not affected by the pH of the drop. This result is reported for both 6P/1F/2Si and 6P/1F surfaces. Consequently, the superhydrophobic character of the 6P/1F/2Si surface is maintained over a wide range of pH, from 0 to 14. A comparable chemical stability was reported by Aslanidou et al. who produced a superamphiphobic coating on the stone using Silres BS29A and SiO₂ NPs [20]. The results of Figure 8b show that both surfaces were highly hydrophobic (WCA > 130°) after 18 weeks of accelerated ageing in the UV chamber. Superhydrophobicity of the 6P/1F/2Si surface was maintained for 2 weeks of treatment and switched to enhanced hydrophobicity for longer treatment periods. The wetting properties of the 6P/1F surface remained practically unchanged, showing the stability of silane-based materials [40] and fluorinated molecules [41].

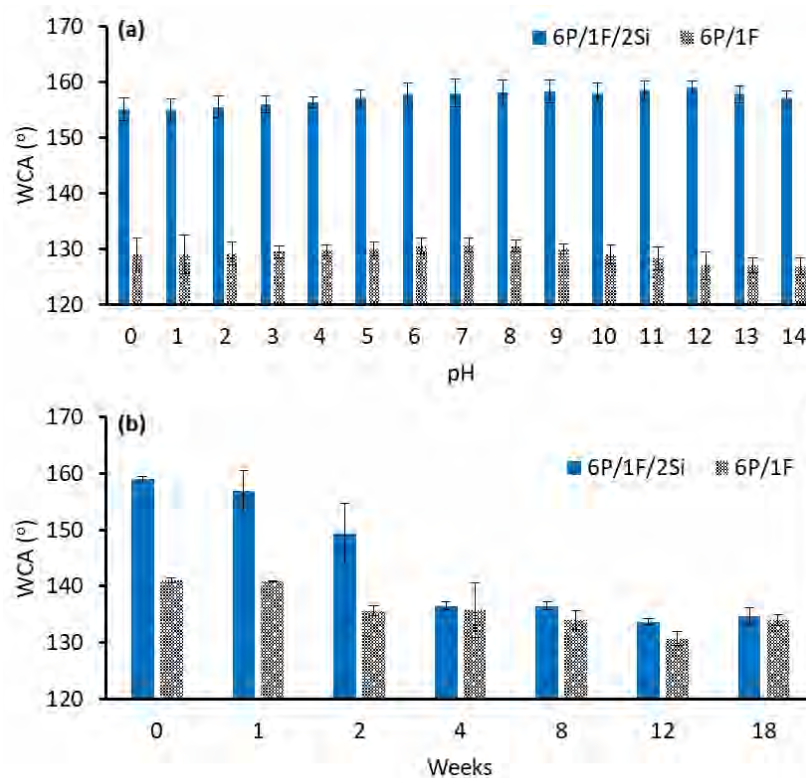


Figure 8. Results for 6P/1F/2Si and 6P/1F surfaces are shown as follows. (a) WCA vs the pH of water drops. (b) WCA for samples which were exposed to artificially accelerated UV radiation for various periods (weeks).

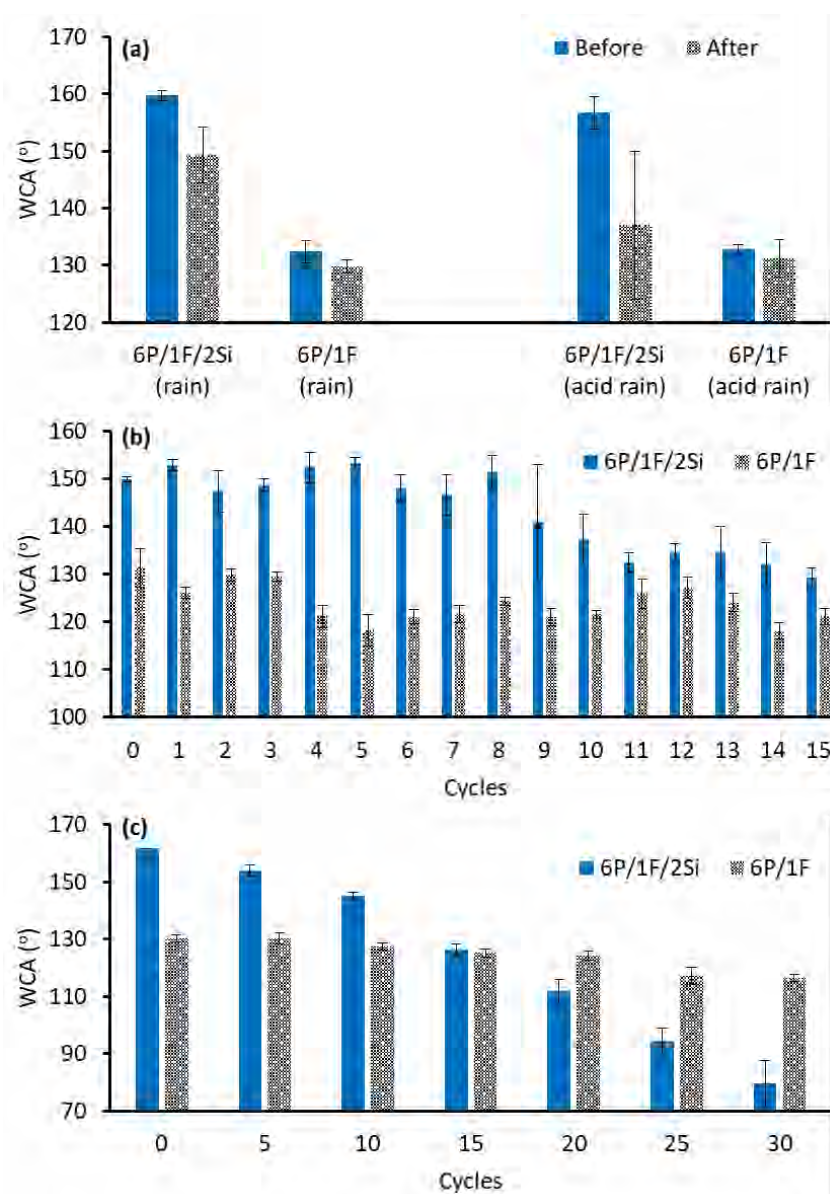


Figure 9. Results for 6P/1F/2Si and 6P/1F surfaces are shown as follows. (a) WCA before and after the rain and the acid rain simulation test. (b) WCA for several freezing and thawing cycles. (c) WCA for several tape peeling cycles.

According to the results of Figure 9a, superhydrophobicity was roughly maintained for the 6P/1F/2Si surface after the application of the simulated rainfall test, whereas WCA on the 6P/1F surface showed only a very slight reduction. Likewise, a superhydrophobic coating that was produced using a water-soluble fluoroalkylsilane product (Dynasylan F8815) and SiO₂ NPs showed good resistivity against water impact [29]. Superhydrophobicity was maintained after placing the sample under a water column which dropped 2500 Lm⁻² of water from a height of 50 cm [29] i.e., treatment conditions were similar to those applied herein. The wetting properties of the 6P/1F surface were practically not affected by acid rain (Figure 9a). However, the results of the same Figure 9a show that the effect of acid rain on the wetting properties of the 6P/1F/2Si surface was pronounced. In particular, WCA reduced from its initial value of 156.7° to 137.0°, after exposing the 6P/1F/2Si surface to acid rain. It is interesting to note that the 137.0° mean value is accompanied by a large variety that is depicted as a long error bar in Figure 9a, indicating that the surface became highly non-uniform. Figure 9b shows that after exposing the two surfaces to 15 harsh freezing and thawing cycles their wetting properties were affected, as

WCAs reduced to 129.2° and 121.2° for the 6P/1F/2Si and 6P/1F surfaces, respectively. The superhydrophobic character of the 6P/1F/2Si was maintained for 8 cycles. It should be noted that the temperature variation applied within the cycle was quite large as the samples were cooled down to the very low temperature of −22 °C and then thawed to room temperature. Despite the harsh conditions, enhanced hydrophobicity (WCA > 120°) was evidenced on both surfaces, after 15 cycles of treatment. In another study, a superamphiphobic (3-perfluoroether-amidopropylsilane) coating designed for the protection of stone was exposed to an artificial environment with fluctuating temperature −5/40 °C and humidity 40/90% [34]. In this study, superhydrophobicity remained practically unchanged after 20 cycles [34]. Figure 9c shows the results of the tape peeling test. Elevated WCA on the 6P/1F/2Si surface was maintained after 15 cycles whereas superhydrophobicity was lost after 5 peeling cycles. WCA dropped substantially after 20 peeling cycles. In another study, good durability of a superhydrophobic nanocomposite coating produced for the protection of stone was reported for 20 attachment-detachment cycles tested [29]. According to Figure 9c, the WCA measurements which were taken after multiple peelings (≥20 cycles) on the 6P/1F/2Si surface were accompanied by large variations, revealing the non-uniform damaging effects of peeling. According to the results of Figure 9c, a less dramatic reduction of WCA with peeling cycles is observed for the 6P/1F surface, which showed better performance (i.e., higher hydrophobicity) compared with the 6P/1F/2Si surface after multiple (≥20) peeling cycles.

3.5. Various Substrates

6P/1F/2Si coatings were applied onto various materials which are used in heritage and modern buildings and constructions, such as sandstone, granite, steel, and copper. Contact angles were measured and the results are summarised in Table 2. Results on coated marble are included in Table 2 which shows that superhydrophobicity and water repellency were achieved on any treated substrate, as evidenced by the large WCA and low contact angle hysteresis of water drops. Coated marble, granite, and steel passed clearly the threshold for superoleophobicity (OCA > 150°) which was almost achieved on coated sandstone and copper. Low contact hystereses of oil drops were measured on the coated materials whereas extreme oil repellency was observed on coated granite and steel. The results of Table 2 show that the developed method is versatile and can be used to impart superamphiphobicity to a wide range of different materials.

Table 2. Contact angle measurements of water and oil drops on various materials coated with 6P/1F/2Si.

Substrate	Water Drop		Oil Drop	
	WCA (°)	Hysteresis (°)	OCA (°)	Hysteresis (°)
Marble	158.0 ± 2.5 *	5.7 ± 0.5	152.2 ± 0.7 *	15.8 ± 1.7
Sandstone	159.6 ± 3.1	3.1 ± 0.6	145.6 ± 6.7	8.9 ± 2.1
Granite	163.2 ± 0.5	2.5 ± 0.6	158.0 ± 2.3	5.6 ± 1.0
Steel	158.1 ± 2.7	3.1 ± 1.1	157.6 ± 6.0	4.6 ± 2.0
Copper	164.0 ± 3.4	2.6 ± 0.7	147.0 ± 1.8	14.5 ± 2.3

* Reproduced from Tables S2 and S3.

4. Conclusions

The main message of this work is that the wetting properties of inherent hydrophobic silane-based materials can obtain superamphiphobic properties when they are mixed with fluoropolymers and silica (SiO₂) nanoparticles to affect simultaneously both surface chemistry and surface morphology. Superamphiphobicity is a highly desirable property for silane-based products, as these are extensively used for the protection of heritage and modern buildings which are threatened by rainwater and oil-based pollutants. It is stressed that these results are reported for the relative concentrations of materials (silane, fluoropolymer, and nanoparticles) which were investigated in this study. As the resulting

coating is highly non-uniform, it is impossible to provide general guidelines to obtain superamphiphobicity which could be applied on any polysiloxane coating blended with a low-surface energy agent and nanoparticles.

In the present study, an aqueous silane solution (Protectosil SC Concentrate) was enriched with a water-based fluoropolymer (C6 fluorocarbon polymer, cationic) emulsion and SiO₂ nanoparticles (7 nm in mean diameter) in various concentrations. The dispersions were sprayed on marble specimens. At appropriate fluoropolymer and nanoparticle concentrations, the produced coatings obtained superamphiphobic properties, as evidenced by the large (>150°) contact angles of water and oil drops. Water and oil repellency was evidenced by the low contact angle hysteresis of both water and oil drops, and moreover, by the results offered by a custom-made device (*Kerberos*) which monitors simultaneously deformation of the liquid interface, spreading and sliding of the droplet along the sample surface during tilting.

A selected superamphiphobic coating, which was prepared using a sol with 6% *w/w* Protectosil, 1% *w/w* Fluoropolymer, and 2% *w/w* SiO₂ (6P/1F/2Si), was subjected to several durability tests in comparison with its hydrophobic counterpart material, prepared without SiO₂ (6P/1F). In particular, contact angles of drops of different pHs, ranging from 0 to 14 were measured on coated marble samples, which were furthermore subjected to freezing-thawing cycles, rain simulation, and acid rain simulation tests and were exposed to artificially accelerated UV ageing. Overall, the 6P/1F/2Si coating showed good resistance against the effects of the harsh conditions of the aforementioned tests. However, the 6P/1F coating showed better performance compared with the 6P/1F/2Si coating after multiple cycles (≥20) of tape peeling. The versatile method can be used to impart superamphiphobicity to various materials, as shown in Table 2.

Supplementary Materials: The following supporting information can be downloaded at: <https://www.mdpi.com/article/10.3390/coatings13040700/s1>, Table S1: aqueous dispersions which were prepared and used in the study to treat marble; Table S2: water contact angle (WCA) measurements; Table S3: oil contact angle (OCA) measurements; Figure S1: SEM-EDX spectrum of fluoropolymer; Figure S2: SEM-EDX spectrum of SiO₂ NPs; Figure S3: self-cleaning scenario.

Author Contributions: Conceptualization, I.K.; methodology, P.N.M., V.T. and I.K.; investigation, P.N.M., Z.C., V.T. and S.P.E.; resources, P.K.S. and T.D.K.; data curation, P.N.M., Z.C., V.T., S.P.E. and I.K.; writing—original draft preparation, I.K.; writing—review and editing, ALL; supervision, P.K.S., T.D.K. and I.K.; project administration, P.K.S.; funding acquisition, P.K.S. and T.D.K. All authors have read and agreed to the published version of the manuscript.

Funding: This research was funded by the program ‘Diagnostic and Preservation Open Lab of Pella’s Palace’ funded by EPAnEK–ESPA 2014-2020 Special Actions “Aquaculture–Industrial Materials–Open Innovation in Culture” (Program code: T6YBII-00069).

Institutional Review Board Statement: Not applicable.

Informed Consent Statement: Not applicable.

Data Availability Statement: The data presented in this study are available on request from the corresponding author.

Conflicts of Interest: The authors declare no conflict of interest.

References

1. Wheeler, G. *Alkoxysilanes and the Consolidation of Stone*; The Getty Conservation Institute: Los Angeles, CA, USA, 2005.
2. Hosseini, M.; Karapanagiotis, I. (Eds.) *Advanced Materials for the Conservation of Stone*; Springer: Cham, Switzerland, 2018.
3. Lampakis, D.; Manoudis, P.N.; Karapanagiotis, I. Monitoring the polymerization process of Si-based superhydrophobic coatings using Raman spectroscopy. *Prog. Org. Coat.* **2013**, *76*, 488–494. [[CrossRef](#)]
4. Fantazzini, P.; Piacenti, F. Hydrophobic treatments for stone conservation - Influence of the application method on penetration, distribution and efficiency. *Stud. Conserv.* **2003**, *48*, 217–226.

5. Crupi, V.; Fazio, B.; Gessini, A.; Kis, Z.; La Russa, M.F.; Majolino, D.; Masciovecchio, C.; Ricca, M.; Rossi, B.; Ruffolo, S.A.; et al. TiO₂-SiO₂-PDMS nanocomposite coating with self-cleaning effect for stone material: Finding the optimal amount of TiO₂. *Constr. Build. Mater.* **2018**, *166*, 464–471.
6. Facio, D.S.; Ordonez, J.A.; Gil, M.A.A.; Carrascosa, L.A.M.; Mosquera, M.J. New consolidant-hydrophobic treatment by combining SiO₂ composite and fluorinated alkoxysilane: Application on decayed biocalcareous stone from an 18th century Cathedral. *Coatings* **2018**, *8*, 170. [[CrossRef](#)]
7. Renda, V.; De Buergo, M.A.; Saladino, M.L.; Caponetti, E. Assessment of protection treatments for carbonatic stone using nanocomposite coatings. *Prog. Org. Coat.* **2020**, *141*, 105515.
8. Yilgör, E.; Yilgör, I. Silicone containing copolymers: Synthesis, properties and applications. *Prog. Polym. Sci.* **2014**, *39*, 1165–1195.
9. Wu, K.H.; Chao, C.M.; Yeh, T.F.; Chang, T.C. Thermal stability and corrosion resistance of polysiloxane coatings on 2024-T3 and 6061-T6 aluminum alloy. *Surf. Coat. Technol.* **2007**, *201*, 5782–5788.
10. Zhang, C.; Qu, L.; Wang, Y.; Xu, T.; Zhang, C. Thermal insulation and stability of polysiloxane foams containing hydroxyl-terminated polydimethylsiloxanes. *RSC Adv.* **2018**, *8*, 9901.
11. Allesandrini, G.; Aglietto, M.; Castelvetro, V.; Ciardelli, F.; Peruzzi, R.; Toniolo, L. Comparative evaluation of fluorinated and nonfluorinated acrylic copolymers as water-repellent coating materials for stone. *J. Appl. Polym. Sci.* **2000**, *76*, 962–977.
12. Rizzarelli, P.; La Rosa, C.; Torrisi, A. Testing a fluorinated compound as a protective material for calcarenite. *J. Cult. Herit.* **2001**, *2*, 55–62. [[CrossRef](#)]
13. Toniolo, L.; Poli, T.; Castelvetro, V.; Manariti, A.; Chiantore, O.; Lazzari, M. Tailoring new fluorinated acrylic copolymers as protective coatings for marble. *J. Cult. Herit.* **2002**, *3*, 309–316. [[CrossRef](#)]
14. Manoudis, P.N.; Karapanagiotis, I.; Tsakalof, A.; Zuburtikudis, I.; Kolinkeova, B.; Panayiotou, C. Superhydrophobic films for the protection of outdoor cultural heritage assets. *Appl. Phys. A Mater.* **2009**, *97*, 351–360.
15. Wenzel, R.N. Resistance of solid surfaces to wetting by water. *Eng. Chem.* **1936**, *28*, 988–994.
16. Cassie, A.B.D.; Baxter, S. Wettability of porous surfaces. *Trans. Faraday Soc.* **1944**, *40*, 546–951.
17. Manoudis, P.N.; Karapanagiotis, I.; Tsakalof, A.; Zuburtikudis, I.; Panayiotou, C. Superhydrophobic composite films produced on various substrates. *Langmuir* **2008**, *24*, 11225–11232.
18. Karapanagiotis, I.; Pavlou, A.; Manoudis, P.N.; Aifantis, K.E. Water repellent ORMOSIL films for the protection of stone and other materials. *Mater. Lett.* **2014**, *131*, 276–279.
19. Barthlott, W.; Neinhuis, C. Purity of the sacred lotus, or escape from contamination in biological surfaces. *Planta* **1997**, *202*, 1–8.
20. Aslanidou, D.; Karapanagiotis, I.; Panayiotou, C. Tuning the wetting properties of siloxane-nanoparticle coatings to induce superhydrophobicity and superoleophobicity for stone protection. *Mater. Des.* **2018**, *2016*, 736–744.
21. Adamopoulos, F.G.; Vouvoudi, E.C.; Pavlidou, E.; Achilias, D.S.; Karapanagiotis, I. TEOS-based superhydrophobic coating for the protection of stone-built cultural heritage. *Coatings* **2021**, *11*, 135. [[CrossRef](#)]
22. Karapanagiotis, I.; Manoudis, P.N. Superhydrophobic and superamphiphobic materials for the conservation of natural stone: An overview. *Constr. Build. Mater.* **2022**, *320*, 126175.
23. Manoudis, P.N.; Karapanagiotis, I.; Tsakalof, A.; Zuburtikudis, I.; Kolinkeová, B.; Panayiotou, C. Surface properties of superhydrophobic coatings for stone protection. *J. Nano Res.* **2009**, *8*, 23–33. [[CrossRef](#)]
24. Manoudis, P.N.; Tsakalof, A.; Karapanagiotis, I.; Zuburtikudis, I.; Panayiotou, C. Fabrication of super-hydrophobic surfaces for enhanced stone protection. *Surf. Coat. Technol.* **2009**, *203*, 1322–1328. [[CrossRef](#)]
25. Chatzigrigoriou, A.; Manoudis, P.N.; Karapanagiotis, I. Fabrication of water repellent coatings using waterborne resins for the protection of the cultural heritage. *Macromol. Symp.* **2013**, *331–332*, 158–165. [[CrossRef](#)]
26. Facio, D.S.; Mosquera, M.J. Simple strategy for producing superhydrophobic nanocomposite coatings in situ on a building substrate. *ACS Appl. Mater. Interfaces* **2013**, *5*, 7517–7526. [[CrossRef](#)]
27. Facio, D.S.; Carrascosa, L.A.M.; Mosquera, M.J. Producing lasting amphiphobic building surfaces with self-cleaning properties. *Nanotechnology* **2017**, *28*, 265601. [[CrossRef](#)]
28. Aslanidou, D.; Karapanagiotis, I.; Lampakis, D. Waterborne superhydrophobic and superoleophobic coatings for the protection of marble and sandstone. *Materials* **2018**, *11*, 585. [[CrossRef](#)]
29. Mosquera, M.J.; Carrascosa, L.A.M.; Badreldin, N. Producing superhydrophobic/oleophobic coatings on cultural heritage building materials. *Pure Appl. Chem.* **2018**, *90*, 551–561. [[CrossRef](#)]
30. Zarzuela, R.; Carbú, M.; Gil, M.L.A.; Cantoral, J.M.; Mosquera, M.J. Ormosils loaded with SiO₂ nanoparticles functionalized with Ag as multifunctional superhydrophobic/biocidal/consolidant treatments for buildings conservation. *Nanotechnology* **2019**, *30*, 345701. [[CrossRef](#)]
31. Cappelletti, G.; Fermo, P.; Camiloni, M. Smart hybrid coatings for natural stones conservation. *Prog. Org. Coat.* **2015**, *78*, 511–516. [[CrossRef](#)]
32. De Ferri, L.; Lottici, P.P.; Lorenzi, A.; Montenero, A.; Salvioli-Mariani, E. Study of silica nanoparticles-polysiloxane hydrophobic treatments for stone-based monument protection. *J. Cult. Herit.* **2011**, *12*, 356–363. [[CrossRef](#)]
33. Stefanidou, M.; Matziaris, K.; Karagiannis, G. Hydrophobization by means of nanotechnology on Greek sandstones used as building facades. *Geosciences* **2013**, *3*, 30–45. [[CrossRef](#)]
34. Cao, Y.; Salvini, A.; Camaiti, M. One-step fabrication of robust and durable superamphiphobic, self-cleaning surface for outdoor and in situ application on building substrates. *J. Colloid Interface Sci.* **2021**, *591*, 239–252. [[CrossRef](#)]

35. Evgenidis, S.P.; Kalic, K.; Kostoglou, M.; Karapantsios, T.D. Kerberos: A three camera headed centrifugal/tilting device for studying wetting/dewetting under the influence of controlled body forces. *Colloids Surf. A Physicochem. Eng. Asp.* **2017**, *521*, 38–48. [[CrossRef](#)]
36. Rios-Lopez, I.; Evgenidis, S.; Kostoglou, M.; Zabulis, X.; Karapantsios, T.D. Effect of initial droplet shape on the tangential force required for spreading and sliding along a solid surface. *Colloids Surf. A Physicochem. Eng. Asp.* **2018**, *549*, 164–173. [[CrossRef](#)]
37. Rios-López, I.; Petala, M.; Kostoglou, M.; Karapantsios, T. Sessile droplets shape response to complex body forces. *Colloids Surf. A Physicochem. Eng. Asp.* **2019**, *572*, 97–106. [[CrossRef](#)]
38. Ting, Y.; Yiping, Z.; Zheng, P.; Wang, L.; Yan, Z.; Ge, D.; Yang, L. Ultra-durable superhydrophobic surfaces from 3D self-similar network via co-spraying of polymer microspheres and nanoparticles. *Chem. Eng. J.* **2021**, *410*, 128314.
39. Jarad, N.A.; Imran, H.; Imani, S.M.; Didar, T.F.; Soleymani, L. Fabrication of superamphiphobic surfaces via spray coating; a review. *Adv. Mater. Technol.* **2022**, *7*, 2101702. [[CrossRef](#)]
40. Striani, R.; Esposito Corcione, C.; Dell'Anna Muia, G.; Frigione, M. Durability of a sunlight-curable organic–inorganic hybrid protective coating for porous stones in natural and artificial weathering conditions. *Prog. Org. Coat.* **2016**, *101*, 1–14. [[CrossRef](#)]
41. Ciardelli, F.; Aglietto, M.; Castelvetro, V.; Chiantore, O.; Toniolo, L. Fluorinated polymeric materials for the protection of monumental buildings. *Macromol. Symp.* **2000**, *152*, 211–222. [[CrossRef](#)]

Disclaimer/Publisher's Note: The statements, opinions and data contained in all publications are solely those of the individual author(s) and contributor(s) and not of MDPI and/or the editor(s). MDPI and/or the editor(s) disclaim responsibility for any injury to people or property resulting from any ideas, methods, instructions or products referred to in the content.